arXiv:1612.00781v1 [cond-mat.str-el] 2 Dec 2016

# Single crystal growth and characterization of $GdRh_2Si_2$

K. Kliemt, C. Krellner

Kristall- und Materiallabor, Physikalisches Institut,
Goethe-Universität Frankfurt, Max-von-Laue Stasse 1,
60438 Frankfurt am Main, Germany

kliemt@physik.uni-frankfurt.de

**Abstract**

High-temperature indium flux growth was applied to prepare single crystals of $GdRh_2Si_2$ by a modified Bridgman method leading to mm-sized single crystals with a platelet habitus. Specific heat and susceptibility data of $GdRh_2Si_2$ exhibit a pronounced anomaly at $T_N = 107\,\mathrm{K}$, where the AFM ordering sets in. Magnetic measurements on the single crystals were performed down to $T = 2\,\mathrm{K}$ in external fields from B = 0 - 9 T applied along the [100]-, [110]- and [001]-direction of the tetragonal lattice. The effective magnetic moment determined from a Curie-Weiss fit agrees well with values from literature, and is larger than the theoretically predicted value. Electrical transport data recorded for current flow parallel and perpendicular to the [001]-direction show a large anisotropy below $T_N$. The residual resistivity ratio $\mathrm{RRR} = \rho_{300\mathrm{K}}/\rho_0 \sim 23$ demonstrates that we succeeded in preparing high-quality crystals using high-temperature indium flux-growth.

## 1 Introduction

Among the ternary silicides of the type $RT_2Si_2$ (R = rare earth, T = transition metal) which crystallize in the body-centered tetragonal $ThCr_2Si_2$ struc-

ture, $GdRh_2Si_2$ has attracted much attention in the last decades as it belongs to the compounds with rare earth elements with exceptional magnetic properties, e.g., $CeRh_2Si_2$ [1], $YbRh_2Si_2$ [2] and $EuRh_2Si_2$ [3, 4]. Studies of Gd-compounds are of special interest since the $4f$ shell of Gd is half filled and therefore its ground state with $S = 7/2$ and $L = 0$ is insensitive to crystal-electric-field (CEF) effects. In the past, polycrystalline $GdRh_2Si_2$ was subject to several investigations. Magnetization and Mössbauer studies were performed by Felner and Nowik [5, 6] examining the series $RRh_2Si_2$ and by Czjzek *et al.* [7] with focus on the properties of the transition metal T in the compounds $GdT_2Si_2$. From Mössbauer spectra of $^{155}$Gd in $GdRh_2Si_2$ it was deduced that the rare earth local moments order antiferromagnetically with the ordering in the basal plane perpendicular to the fourfold symmetry axis of the tetragonal lattice [5, 6]. It is known from neutron diffraction experiments, that the antiferromagnetic properties in the series $RRh_2Si_2$ arise due to a stacking of ferromagnetic layers [8]. Pressure studies by Szytuła *et al.* [9] revealed that the Néel temperature of $GdRh_2Si_2$ decreases with increasing applied pressure. An ESR-study was performed by Kwapulinska *et al.* [10] and they found that the $g$-factor is temperature independent from $T_N$ to 300 K with $g = 1.995 \pm 0.01$. Recently, the magnetic properties of $GdRh_2Si_2$ were investigated by hyperfine interactions and magnetization measurements [11].

All measurements up to now were carried out on polycrystalline material since single crystals were not available. Here, we report on the successful crystal growth and present a detailed study of the magnetic and electrical transport properties of $GdRh_2Si_2$ single crystals. The crystals were grown using a high-temperature indium-flux technique [13, 12]. The crystal growth set up was chosen similarly to that applied for the single crystal growth of $YbRh_2Si_2$ [14].

# 2 Experimental details

Single crystals of $GdRh_2Si_2$ were grown in In flux. The high purity starting materials Gd (99.9%, Johnson Matthey), Rh (99.9%, Heraeus), Si (99.9999%, Wacker), with the molar ratio of 1:2:2, and In (99.9995%, Schuckard) were weighed in a graphite crucible and sealed in a tantalum crucible under argon atmosphere (99.999%). The stoichiometric composition of the elements was used with 96at% indium as flux. The experimental setup of the crucible is

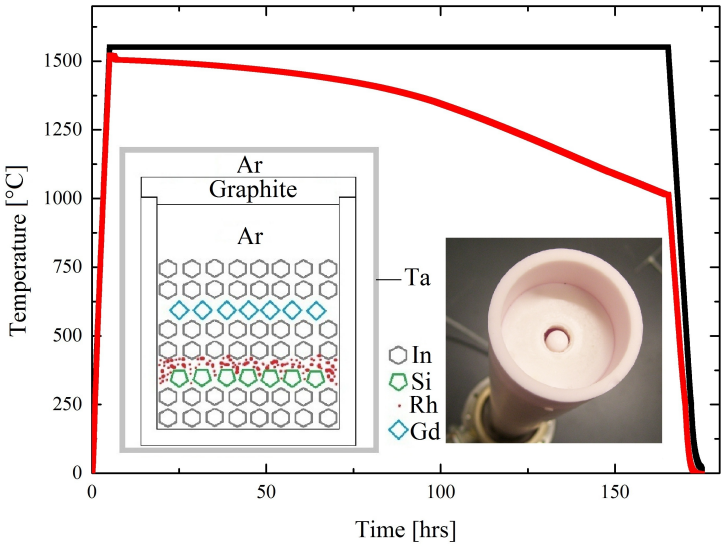


Figure 1: Measured temperature-time-profiles for a growth experiment (red curve) and furnace temperature (black curve). Inset on the right: Picture of the platform on which the crucible is mounted during the growth. The temperature was measured with a thermocouple directly at the bottom of the crucible. Inset on the left: Schematic arrangement of the elements in the crucible system for the crystal growth of $GdRh_2Si_2$. The inner crucible is made from graphite, enclosed under argon in a Ta-crucible.

shown in the left inset of Figure 1. Indium was put on the bottom of the crucible covered by the high-melting elements Rh and Si covered again by In pieces. Subsequently, the crucible was transfered to the Ar-filled glove-box, where Gd was placed on top, covered once more by In. Finally, the Ta-crucible was closed using arc-welding. The filled Ta-crucible was put under a stream of Ar in a resistive furnace (GERO HTRV 70-250/18) and the elements were heated up to 1550°C. The melt was homogenized for 1 hrs and than cooled by slowly moving the whole furnace leading to a cooling rate of 1 mm/hrs down to 1000°C, while the position of the crucible stayed fixed. During the growth, the temperature was measured at the bottom of the tantalum crucible by a thermocouple of type B. In figure 1 the recorded temperature-time profile is depicted. The crucible holder made from $Al_2O_3$ together with the tip of the thermocouple in the center is shown in the right inset. After the growth, the excess flux was removed with diluted

HCl. The crystal structure was characterized by powder X-ray diffraction on crushed single crystals, using Cu-$K_\alpha$ radiation. The chemical composition was checked by energy-dispersive X-ray spectroscopy (EDX). The orientation of the single crystals was determined using a Laue camera with X-ray radiation from a tungsten anode. Four-point resistivity, magnetization, and heat-capacity measurements were performed using the commercial measurements options of a Quantum Design PPMS.

# 3 Results and discussion

## 3.1 Crystal growth

Until now, the successful single crystal growth was not reported, which probably is due to the incongruently melting of this material at temperatures above 2000°C. We therefore employed the flux-growth technique, which allows to perform the crystal growth at temperatures below the high melting points of the elements (Gd 1312°C, Rh 1964°C, and Si 1414°C). So far, it was not possible to determine the accurate crystallization temperature of $GdRh_2Si_2$ in 96 at% In, but a systematic optimization of the starting temperature revealed that the largest crystals could be grown when starting the crystal growth at $T_{start}$= 1520°C, compared to growths starting below 1500°C. The optimized temperature-time profile is depicted in Fig. 1.

After cooling, the excess In is dissolved by hydrochloric acid, which removes binary Rh-In compounds as well. The formation of the latter, indicates that the initial stoichiometry of the melt needs still to be optimized. However, the resulting single crystals of $GdRh_2Si_2$ are already large enough to carry out several physical characterization measurements as described above. A typical single crystal has a platelet habitus with the shortest dimension, 200-500$\mu$m, along the crystallographic $c$-direction, as shown in Fig. 2a.

## 3.2 Structural and chemical characterization

The single crystals were analyzed with electron microscopy and the secondary electron image indicates the absence of any inclusions of secondary phases (Fig. 2b). From that picture, the formation of terraces along the $c$-direction is apparent. The chemical composition determined by EDX microprobe analysis revealed (20±1)at.% Gd, (40±1)at.% Rh and (40±2)at.% Si. Powder

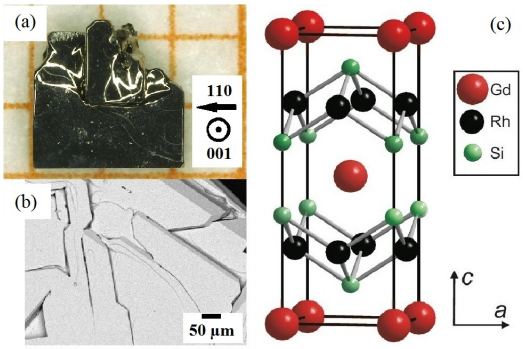


Figure 2: (a) Optical microscope image of a $GdRh_2Si_2$ single crystal. The largest crystal edges always belong either to the [100]- or the [110]-direction; (b) Electron microscopy (secondary electrons) indicates the phase purity of the crystal; (c) Tetragonal crystal structure of $GdRh_2Si_2$.

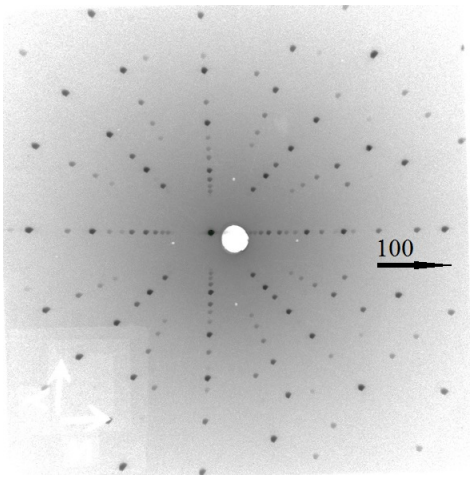


Figure 3: The Laue pattern of the 001-direction shows the 4-fold symmetry. The sharp reflexes are an indicator for the good sample quality.

X-ray diffraction measurements confirmed the $I4/mmm$ tetragonal structure (Fig. 2c) with lattice parameters a = 4.042(2) Å and c = 9.986(4) Å, which is in agreement with the data published for polycrystalline samples [5, 9, 11].

The high quality of the single crystals is evident also from a Laue back scattering image, presented in Fig. 3. The central point can be indexed as the (001) reflex, proving that the direction perpendicular to the surface of the platelets corresponds to the $c$-direction. The sharp points verify, that the terraces seen in Fig. 2b do not lead to a slight misalignment along $c$.

## 3.3 Specific-heat measurements

In Fig. 4 specific-heat data are shown for the two related materials $GdRh_2Si_2$ and $LuRh_2Si_2$. The latter serves as a non-magnetic reference system with a completely filled $4f-$shell and the data are taken from Ref. [15]. For $GdRh_2Si_2$ a pronounced and sharp $\lambda$-type anomaly is observed at $T_N$, establishing a second order phase transition into the AFM ordered phase. For $T <$ 5 K the specific heat of $GdRh_2Si_2$ can be well described by $C/T = \gamma_0 + \beta T^2$ (cf. inset of Fig. 4) with the Sommerfeld coefficient $\gamma_0 \approx 4\mathrm{mJ/molK^2}$ determined from a linear fit to the data. The Debye temperature $\Theta_D \approx 148\,\mathrm{K}$ was calculated from the slope $\beta$ according to $\beta = 12\pi^4 R/(5\Theta_D^3)$.

## 3.4 Magnetic measurements

In Fig. 5 susceptibility data as a function of temperature is presented for one single crystal with the magnetic field along the [100]-direction. At small fields ($B \leq 0.1\,\mathrm{T}$) a sharp anomaly is evident at $T_N = 107\,\mathrm{K}$ followed by a strong decrease towards lower temperatures. At higher magnetic fields, $0.1\mathrm{T} < B < 1\,\mathrm{T}$, a field-induced anomaly emerges below $T_N$ shifting to lower temperatures with increasing field, visible e.g. as a pronounced drop at $T^* = 50\,\mathrm{K}$ for $B = 0.5\,\mathrm{T}$. Above 1 T, the susceptibility is nearly field independent, and slightly increases with decreasing temperature. This behavior is different for different field directions, as shown in the inset of Fig. 5. Here, $\chi(T)$ is shown for $B = 0.1\,\mathrm{T}$ with $B \parallel 100$ (blue open triangles), $B \parallel 110$ (black open squares), $B \parallel 001$ (red closed squares), and $B$ aligned in an angle of 22.5° to the [100]- and the [110]-direction as well as perpendicular to the [001]-direction (green closed squares). Remarkably for $B \parallel 001$ and $B \parallel 110$, $\chi(T)$ is changing only slightly below $T_N$ in contrast to the strong decrease

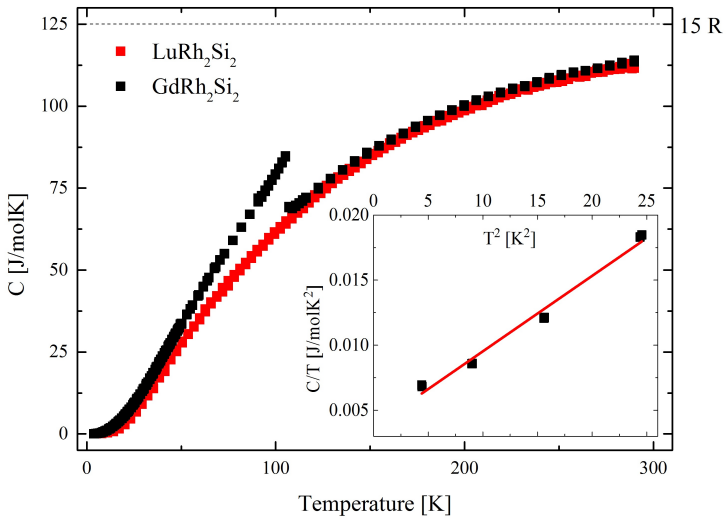


Figure 4: Specific-heat data as function of temperature for a single crystal of $GdRh_2Si_2$ and polycrystalline $LuRh_2Si_2$ (from Ref. [15]). The inset enlarges the low-temperature part of the specific heat of $GdRh_2Si_2$, plotted as $C/T$ versus $T^2$. From a linear fit, the Sommerfeld coefficient and the Debye temperature could be extracted.

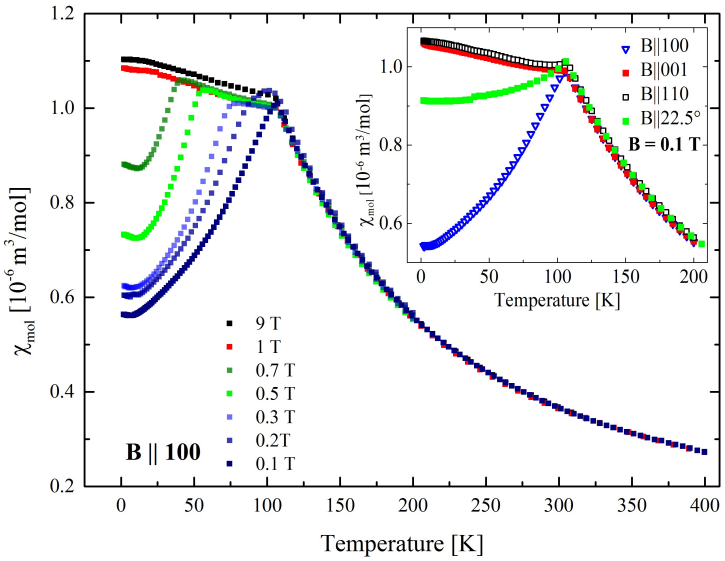


Figure 5: Susceptibility as a function of temperature for B‖100. The spin flop transition shifts towards lower temperatures for higher fields. Inset: Comparison of susceptibility data for an applied field of 0.1 T for 4 different crystal orientations.

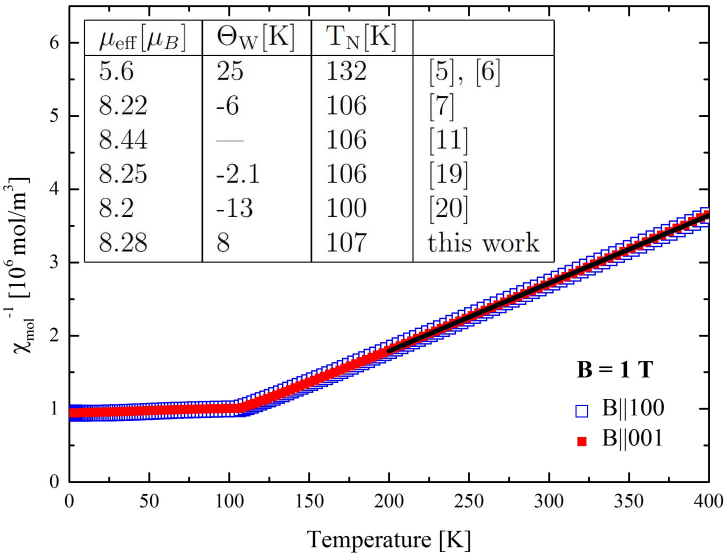


Figure 6: The figure shows the fit of the inverse susceptibility (black solid line) from which the effective magnetic moment and the Weiss temperature were determined.

discussed for $B \parallel 100$. The field direction between the [100]- and the [110]-direction, was measured to prove, that no other in-plane direction shows a more pronounced drop at $T_N$.

Above 150 K, the susceptibility follows a Curie-Weiss behaviour for all measured crystal orientations. The effective magnetic moment, $\mu_{\text{eff}} = (8.28 \pm 0.10)\mu_B$, agrees well with published values determined on polycrystalline samples [7, 18], and is larger than expected for sole $Gd^{3+}$ ions (7.94 $\mu_B$). Furthermore, no anisotropy of the inverse susceptibility above $T_N$ could be resolved in our measurements on single crystals.
The Weiss temperature, $\Theta_W$, was determined from a linear fit of the inverse susceptibility $\chi^{-1}$ from 200 - 400 K, shown as solid black line in Fig. 6, which is positive indicating dominantly ferromagnetic exchange interactions, with $\Theta_W = (8 \pm 5)$K. This is in contrast to the findings of [7, 18] and [19] who reported negative Weiss temperatures. In the inset of Fig. 6 these reported values of the effective magnetic moment $\mu_{\text{eff}}$ and the Weiss temperature $\Theta_W$ are summarized together with our findings.

It is known from earlier work on $RRh_2Si_2$ compounds [8] that antiferromagnetic properties in this family arise due to a stacking of ferromagnetic

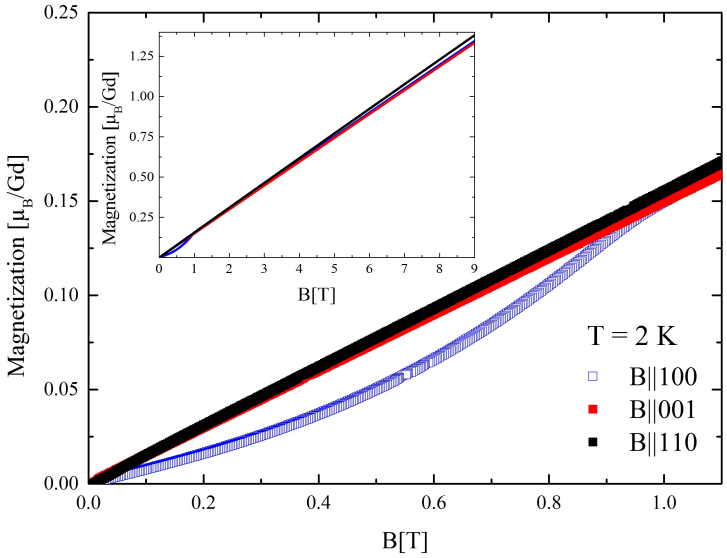


Figure 7: M(B) data for field applied in 3 different crystal orientations at T = 2 K; Spin flop in [100]-direction.

layers. From a Mössbauer experiment was deduced that the magnetic moments in $GdRh_2Si_2$ are aligned in the basal plane of the tetragonal structure [6]. In our measurements we found, that there is a sizeable in-plane anisotropy in $M(T)$ and $M(B)$, Fig. 5 and 7, from which the in-plane alignment of the moments can be deduced. In Fig. 7, $M(B)$ measured for different field directions at $T = 2\,\mathrm{K}$ on a $GdRh_2Si_2$ single crystal is shown. For the field applied parallel to the [100]-direction a small spin flop transition can be observed at $B_{sf} \approx 1\,\mathrm{T}$.

In previous work, some of the compounds $RRh_2Si_2$ were examined by Felner and Nowik [5, 6]. They deduced from magnetization and Mössbauer studies that these compounds have two magnetic phase transitions: one corresponding to the ordering of the rare earth ion and the other one to the itinerant electron ordering of the Rh sublattice. A peak in the susceptibility at about 16 K besides the transition into the AFM ordered state was reported.

The compounds $GdT_2Si_2$ (T = transition metal) were studied by Czjzek et al. [7] by means of Mössbauer spectroscopy and magnetization measurements. In contrast to Felner and Nowik [5, 6], these authors reported that the transition metal ions, with the exception of manganese, do not carry magnetic

moments in any of these compounds. They found an enhanced effective magnetic moment of the $Gd^{3+}$-ions, and proposed the magnetic moments of rare-earth $5d$ electrons induced by $4f$-$5d$ exchange interaction, to be the origin of this additional contribution to the effective moment. XMCD-measurements are presently on the way to answer the question, if the enhancement of the magnetic moment, determined for the $Gd^{3+}$-ions in $GdRh_2Si_2$, results from a contribution of Gd $5d$ electrons.

Furthermore, a hint to the existence of a second magnetic transition at $T_{\mathrm{II}} = 17\,\mathrm{K}$ was reported in Ref. [7]. This statement of Ref. [5, 6] and [7] was based on the observation of a cusp in the susceptibility, similar to what we observe for $B \parallel 100$ at about 0.7 T. We have demonstrated, that this additional cusp is a field-induced transition, due to the spin flop transition at $B_{sf}$, which of course is present in a polycrystalline sample as well, if the magnetic field is in a similar range.

## 3.5 Electrical-transport measurement

$GdRh_2Si_2$ is a tetragonal antiferromagnet with a layered crystal structure (cf. Fig. 2). Here, we report on electrical transport measurements on a $GdRh_2Si_2$ single crystal, with current parallel and perpendicular to the crystallographic $c$-direction. The temperature dependence of the electrical resistivity, $\rho(T)$, for these two current directions is presented in figure 8. The absolute value for the in-plane resistivity j $\perp$001 at room temperature was about 75 $\mu\Omega$cm. Irregularities in the cross section of the sample made it impossible to estimate a reliable absolute value for current flow parallel to the [001]-direction, therefore we present for this direction only the relative values, $\rho/\rho_{300\mathrm{K}}$. For both directions, the resistivity shows a linear-in-temperature behavior from $T = 300\,\mathrm{K}$ down to the AFM phase transition. At $T_N \approx 107$ K a change of the slope in the resistivity curves occurs. Below $T_N$, the decrease of the resistivity becomes stronger if the current flows perpendicular to the [001]-direction. For j parallel to the [001]-direction, the resistivity increases below $T_N$ and drops down after reaching a maximum at about $T = 90\,\mathrm{K}$. This can be understood as a change of the Fermi surface since the periodicity in the lattice becomes larger when entering the AFM phase. In result, more states near the Fermi level that contribute to the conductivity exist for current perpendicular to the [001]-direction and less for current parallel to the [001]-direction. In comparison to previous work [20], where electrical transport measurements were performed on a polycrystalline sample

of $GdRh_2Si_2$ with $\rho_{200K}/\rho_{1.8K} \approx 9$, the sample quality was improved with $RR_{1.8K} = \rho_{300K}/\rho_{1.8K} \approx 23$ ($\rho_{200K}/\rho_{1.8K} \approx 17$) determined for the j $\perp$001-direction of the single crystals.

# 4 Summary

Single crystals of $GdRh_2Si_2$ were grown by a modified Bridgman method from indium flux. The optimization of the temperature profile during the growth led to mm-sized single crystals with a platelet habitus. The specific heat of $GdRh_2Si_2$ shows a sharp $\lambda$-type anomaly at $T_N = 107\,\mathrm{K}$, establishing a second order phase transition into the AFM ordered phase. The data can be described by $C/T = \gamma_0 + \beta T^2$ with the Sommerfeld coefficient $\gamma_0 \approx 4\mathrm{mJ/molK}^2$ for $T < 5$ K. The Debye temperature $\Theta_D \approx 148\,\mathrm{K}$ was determined from the slope $\beta$ of the linear fit. The effective magnetic moment $\mu_{\mathrm{eff}} = (8.28 \pm 0.10)\mu_B$ agrees well with values from literature, and is larger than the theoretically predicted value of $\mu_{\mathrm{eff}} = 7.94\mu_B$. The determined Weiss temperature, $\Theta_{\mathrm{W}} = (8 \pm 5)\,\mathrm{K}$, is much smaller than $T_N$, indicating a pronounced competition between antiferromagnetic and ferromagnetic interactions. Electrical transport data show a large anisotropy for current flow parallel and perpendicular to the [001]-direction below $T_N$. The residual resistivity ratio $RRR = \rho_{300\mathrm{K}}/\rho_0 \sim 23$ shows that we succeeded in growing high-quality crystals from a high-temperature indium flux.

# 5 Acknowledgements

We thank C. Geibel, K. Kummer, and D. V. Vyalikh for valuable discussions and K.-D. Luther for technical support.

# References

[1] S. Quezel, J. Rossat-Mignod, Solid State Commun. **49** (1984) 685 - 691.

[2] O. Trovarelli, C. Geibel, S. Mederle, C. Langhammer, F.M. Grosche, P. Gegenwart, M. Lang, G. Sparn, F. Steglich, Phys. Rev. Lett. **85** (2000) 626-629.

[3] S. Seiro, C. Geibel, J.Phys.: Condens. Matter **26** (2014) 046002.

[4] A. Chikina, M. Höppner, S. Seiro, K. Kummer, S. Danzenbächer, S. Patil, A. Generalov, M. Güttler, Yu. Kucherenko, E.V. Chulkov, Yu. M. Koroteev, M. Köpernik, C. Geibel, M. Shi, M. Radovic, C. Laubschat, D.V. Vyalikh, Nat. Commun., (2014) DOI: 10.1038/ncomms4171.

[5] I. Felner, I. Nowik, Solid State Commun. **47** (1983) 831-834.

[6] I. Felner, I. Nowik, J. Phys. Chem. Solids **45** (1984) 419-426.

[7] G. Czjzek, V. Oestreich, H. Schmidt, K. Łatka, K. Tomala, J. Magn. Magn. Mater. **79** (1989) 42-56.

[8] M. Slaski, J. Leciejewicz, A. Szytuła, J. Magn. Magn. Mater. **39** (1983) 268-274.

[9] A. Szytuła, A. Budkowski, M. Slaski, R. Zach, Solid State Commun. **57** (1986) 813-815.

[10] E. Kwapulinska, K. Kaczmarska, A. Szytuła, J. Magn. Magn. Mater. **73** (1988) 65-68.

[11] G.A. Cabrera-Pasca, A.W. Carbonari, R.N. Saxena, B. Bosch-Santos, J.A.H. Coaquira, J.A. Filho, J. Alloy. Compd. **515** (2012) 44-48.

[12] P.C. Canfield, I.R. Fisher, J. Cryst. Growth **225** (2001) 155-161.

[13] P.C. Canfield, Z. Fisk, Phil. Mag. B **65** (1992) 1117-1123.

[14] C. Krellner, S. Taube, T. Westerkamp, Z. Hossain, C. Geibel, Phil. Mag. **92** (2012) 2508-2523.

[15] J. Ferstl, New Yb-based systems: From an intermediate-valent to a magnetically ordered state, Cuvillier Göttingen (2007).

[16] K.H.J. Buschow, F.R. de Boer, Physics of Magnetism and Magnetic Materials, Kluwer Academic Publishers (2003)

[17] A. Nakamura, Y. Hiranaka, M. Hedo, T. Nakama, Y. Miura, H. Tsutsumi, A. Mori, K. Ishida, K. Mitamura, Y. Hirose, K. Sugijama, F. Honda, R. Settai, T. Takeuchi, M. Hagiwara, T.D. Matsuda, E. Yamamoto, Y. Haga, K. Matsubayashi, Y. Uwatoko, H. Harima, Y. Onuki, J. Phys. Soc. Jpn. **82** (2013) 104703.

[18] L.D. Tung, J.J.M. Franse, K.H.J. Buschow, P.E. Brommer, N.P. Thuy, J. Alloy. Compd. **260** (1997) 35-43.

[19] A. Szytuła, J. Less-Common Met. **157** (1990) 167-171.

[20] G.A. Cabrera-Pasca, A.W. Carbonari, B. Bosch-Santos, J. Mestnik-Filho, R. N. Saxena, J. Phys. Condens. Matter **24** (2012) 416002.

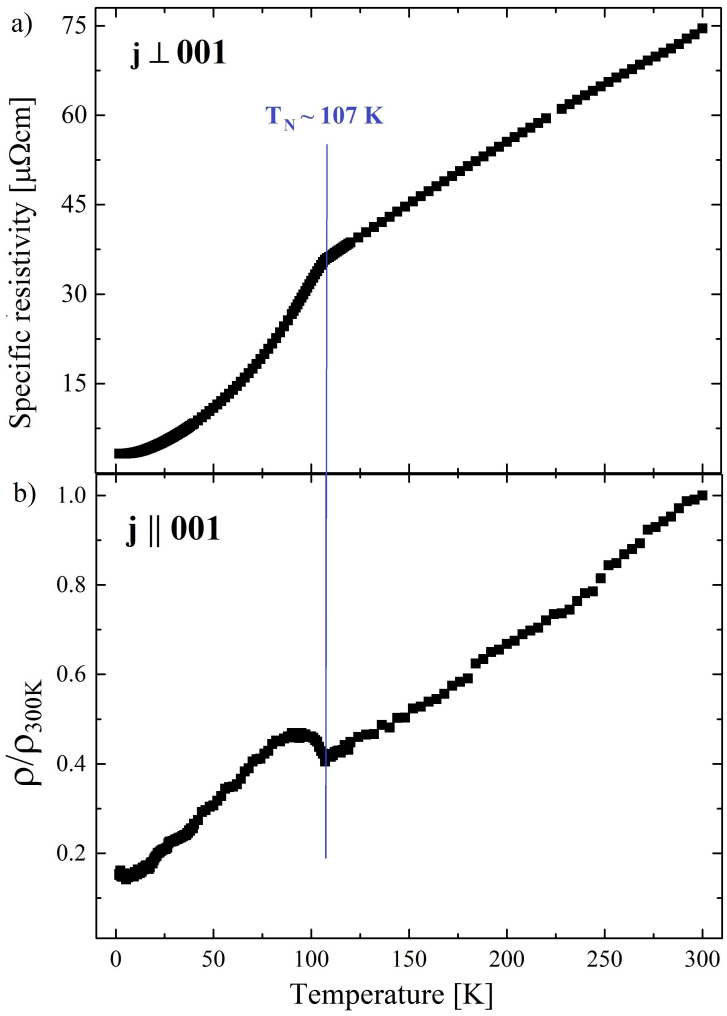


Figure 8: Electrical resistivity measured for current flow a) perpendicular and b) parallel to the [001]-direction. A clear anomaly is visible at $T_N$ which is rather anisotropic for the two current directions.